

# A Modification of Deriche's Approach to Edge Detection

Stefan Lanser, Wolfgang Eckstein

Technische Universität München  
Institut für Informatik, Lehrstuhl Prof. Radig

## Abstract

In 1983 Canny presented criteria for measuring the quality of edge detectors and derived an optimal FIR-Filter for step edges by optimizing them. Four years later Deriche proposed an approach to edge detection based on Canny's design utilizing IIR-Filters which can be implemented very efficiently recursively. Unfortunately, using the Deriche-Filter leads to a distortion of the amplitudes of the edges depending on their direction. In this paper, it will be shown that these distortions are systematic errors which can be eliminated by a simple modification of the edge detection procedure. Because of its obvious "kinship" to the Deriche-filter the Shen-filter has been included in the investigations.

## 1: Deriche's Approach to Edge Detection

Deriche's approach to the detection of step edges ([4]-[6]) is based on Canny's filter design ([1],[2]). Canny had derived an optimal one-dimensional Finite Impulse Response filter for step edges by optimizing specific criteria for the quality of edge detectors. Deriche used the same method to construct an Infinite Impulse Response edge filter. His edge detector performs the following three steps:

- (i) Calculation of  $E_x(x,y)$  by folding the image with the separable 2D-filter  $f(x)g(y)$ .
- (ii) Calculation of  $E_y(x,y)$  by folding the image with the separable 2D-filter  $g(x)f(y)$ .
- (iii) Calculation of the amplitude and the direction of the edge as the length and the orientation of the vector  $[E_x(x,y), E_y(x,y)]^T$ .

In the algorithm above  $f(z)$  stands for a one-dimensional IIR-edge filter and  $g(z)$  for the one-dimensional smoothing filter obtained by integrating  $f(z)$ .  $[E_x(x,y), E_y(x,y)]^T$  is the gradient of the image after folding with the 2D-smoothing filter  $G(x,y) = g(x)g(y)$  (as

shown in [7]). Thus Deriche's approach can be seen as a gradient scheme. Deriche's optimal 1D-edge filter has the following impulse response function:

$$f(z) = K e^{-\alpha|z|} \sin(\omega z), \quad \alpha, \omega > 0.$$

The two most interesting embodiments of this filter,  $f_{D1}(z)$  and  $f_{D2}(z)$ , have been investigated in our project:

$$f_{D1}(z) = K_{D1} z e^{-\alpha|z|} \quad (\omega \ll \alpha),$$

$$f_{D2}(z) = K_{D2} \sin(\alpha z) e^{-\alpha|z|} \quad (\omega = \alpha).$$

$f_{D1}(z)$  is optimal according to Canny's criteria of quality. It has been used by Deriche himself in later works, too ([6]). The filter  $f_{D2}(z)$  is similar to Canny's edge filter in terms of the values of the criterions of quality obtained. Its application leads to far less distortions of amplitudes in the two-dimensional case, which will be shown later. Plugging in  $f_{D1}(z)$  and  $f_{D2}(z)$  in the sketch of the algorithm for edge detection above, the 2D-edge operators  $D1$  and  $D2$  are obtained. The continuous normalizing factors  $K_{D1}$  and  $K_{D2}$  have to be set to

$$K_{D1} = -\alpha_{D1}^2, \quad K_{D2} = -2\alpha_{D2},$$

the discrete factors to

$$K_{D1} = -\frac{(1 - e^{-\alpha_{D1}})^2}{e^{-\alpha_{D1}}}, \quad K_{D2} = -\frac{1 - 2 \cos(\alpha_{D2}) e^{-\alpha_{D2}} + e^{-2\alpha_{D2}}}{\sin(\alpha_{D2}) e^{-\alpha_{D2}}}.$$

Shen's one-dimensional IIR-edge filter ([3]) has been investigated, too:

$$f_S(z) = \left\{ \begin{array}{l} K_S e^{-\alpha_S z}, \quad z > 0 \\ 0, \quad z = 0 \\ -K_S e^{\alpha_S z}, \quad z < 0 \end{array} \right\},$$

where

$$K_S = -\alpha_S \text{ (continuous)}, \quad K_S = -\frac{1 - e^{-\alpha_S}}{e^{-\alpha_S}} \text{ (discrete)}.$$

This filter can be derived from Canny's criteria as well simply by dropping the constraint which reduces the pro-

bability of multiple responses of the filter to one edge. Embedded in Deriche's approach Shen's filter has contributed the S-Operator to our investigation.

The "core" of all examined filters (i.e. the part where the impulse response function differs significantly from zero) is increased with decreasing  $\alpha$ . On the one hand, the smoothing impact of the filters and as a consequence the invariance to noise is increased by this. On the other hand, the resolution for details in the image diminishes. The accompanying 1D-smoothing filters  $g_{D1}(z)$ ,  $g_{D2}(z)$  and  $g_S(z)$  can be derived from  $f_{D1}(z)$ ,  $f_{D2}(z)$  and  $f_S(z)$  by integration. Details about the derivation of all these filters are included in [7].

The discrete forms of the one-dimensional IIR-filters in this paper can be implemented very efficiently. Let  $x(n)$  be the one-dimensional signal to be filtered. Then the filtered output signal  $y(n)$  is obtained by means of the following recursive scheme for calculation:

$$y^+(n) = \sum_{k=0}^{K^+} a_k^+ x(n-k) - \sum_{k=1}^L b_k y^+(n-k),$$

$$y^-(n) = \sum_{k=0}^{K^-} a_k^- x(n+k) - \sum_{k=1}^L b_k y^-(n+k),$$

$$y(n) = C[y^+(n) + y^-(n)].$$

For the examined filters the following values have to be plugged in (see [6],[7]):

$f_{D1}$ :

$$K^- = K^+ = 1, \quad a_k^- = -a_k^+, \quad a_0^+ = 0, \quad a_1^+ = 1,$$

$$L = 2, \quad b_1 = -2e^{-\alpha D1}, \quad b_2 = e^{-2\alpha D1}, \quad C = -(1 - e^{-\alpha D1})^2.$$

$g_{D1}$ :

$$K^+ = 1, \quad a_0^+ = 1, \quad a_1^+ = (\alpha_{D1} - 1)e^{-\alpha D1},$$

$$K^- = 2, \quad a_0^- = 0, \quad a_1^- = (\alpha_{D1} + 1)e^{-\alpha D1}, \quad a_2^- = -e^{-2\alpha D1},$$

$$L = 2, \quad b_1 = -2e^{-\alpha D1}, \quad b_2 = -a_2^-, \quad C = \frac{(1 - e^{-\alpha D1})^2}{1 + 2\alpha_{D1}e^{-\alpha D1} - e^{-2\alpha D1}}.$$

$f_{D2}$ :

$$K^- = K^+ = 1, \quad a_k^- = -a_k^+, \quad a_0^+ = 0, \quad a_1^+ = 1,$$

$$L = 2, \quad b_1 = -2 \cos(\alpha_{D2})e^{-\alpha D2}, \quad b_2 = e^{-2\alpha D2}, \quad C = -1 - b_1 - b_2.$$

$g_{D2}$ :

$$K^+ = 1, \quad a_0^+ = 1, \quad a_1^+ = [\sin(\alpha_{D2}) - \cos(\alpha_{D2})]e^{-\alpha D2}, \quad K^- = 2,$$

$$a_0^- = 0, \quad a_1^- = [\sin(\alpha_{D2}) + \cos(\alpha_{D2})]e^{-\alpha D2}, \quad a_2^- = -e^{-2\alpha D2},$$

$$L = 2, \quad b_1 = -2 \cos(\alpha_{D2})e^{-\alpha D2}, \quad b_2 = -a_2^-,$$

$$C = \frac{1 + b_1 + b_2}{1 + 2 \sin(\alpha_{D2})e^{-\alpha D2} - b_2}.$$

$f_S$ :

$$K^- = K^+ = 1, \quad a_0^- = a_0^+ = 0, \quad a_1^+ = 1, \quad a_1^- = -1,$$

$$L = 1, \quad b_1 = -e^{-\alpha S}, \quad C = -(1 - e^{-\alpha S}).$$

$g_S$ :

$$K^+ = 0, \quad a_0^+ = 1, \quad K^- = 1, \quad a_0^- = 0, \quad a_1^- = e^{-\alpha S},$$

$$L = 1, \quad b_1 = -a_1^-, \quad C = \frac{1 - e^{-\alpha S}}{1 + e^{-\alpha S}}.$$

The main advantage of a recursive implementation (compared with a conventional calculation of the filter output  $y(n)$  by means of filter masks) is the independence of the "size" (the catchment area) of the filters and the computational load for their application. The latter remains constant for arbitrary values of the filter parameters  $\alpha_{D1}$ ,  $\alpha_{D2}$  and  $\alpha_S$  (Shen's filters  $f_S$  and  $g_S$  proved to be most efficient). The catchment area of the filters can be enlarged with no additional expenditures in the application or implementation of the filters just by adjusting the values of the filter parameters. Of course the resulting runtime advantage compared with an implementation using filter masks increases with larger catchment areas of the filters.

## 2: The Amplitude-Distortions of the Operators D1, D2, and S

As mentioned above all of the three operators D1, D2 and S calculate the gradient of the operator-specific smoothed input image. Unfortunately, the 2D-smoothing filters  $G_{D1}(x,y) = g_{D1}(x)g_{D1}(y)$  and  $G_{D2}(x,y) = g_{D2}(x)g_{D2}(y)$  based on Deriche's edge filters and the 2D-smoothing filter  $G_S(x,y) = g_S(x)g_S(y)$  based on Shen's edge filter prove to be anisotropic ( $G_{D1}$  and  $G_S$  significantly,  $G_{D2}$  not too much). This leads to systematic distortions of the amplitudes of edges detected by the operators D1, D2 and S (depending on the directions of the edges). A similar behaviour can be observed in many other gradient techniques for edge detection, too. The examination of these errors in the continuous case is the basis for a modification of the operators eliminating the distortions. Consider the application of the operators (in their continuous form) to an ideal, infinitely extended step edge  $K^\varphi(x,y)$ ,

$$K^\varphi(x,y) = \begin{cases} A, & x \tan \varphi \leq y, \\ 0, & \text{else} \end{cases}$$

with amplitude  $A$  and orientation  $\varphi$ . The operators calculate the amplitudes  $A'$ ,  $A' = V(\varphi) A$ . The direction-sensitive distortions of the original amplitudes,  $V(\varphi)$ , can be shown to be:

$$V(\varphi) = \sqrt{X(\varphi)^2 + Y(\varphi)^2},$$

where the subterms  $X(\varphi)$  and  $Y(\varphi)$  are:

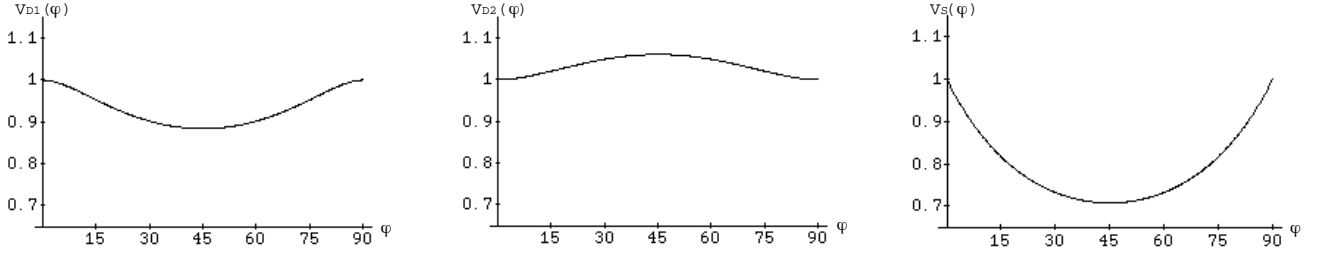


**Figure 1.** The amplitude-distortions of the operators D1 (left), D2 (middle) and S (right) for edge

directions between 0° and 90° (90° and 180° respectively).

$$X_{D1}(\varphi) = 1 - \frac{1}{(1 + \tan \varphi)^2} - \frac{\tan \varphi}{(1 + \tan \varphi)^3},$$

$$Y_{D1}(\varphi) = 1 - \frac{1}{(1 + \cot \varphi)^2} - \frac{\cot \varphi}{(1 + \cot \varphi)^3},$$

$$X_{D2}(\varphi) = 1 - \frac{1}{2(1 + \tan \varphi)} - \frac{1 - \tan \varphi}{2(1 + \tan^2 \varphi)},$$

$$Y_{D2}(\varphi) = 1 - \frac{1}{2(1 + \cot \varphi)} - \frac{1 - \cot \varphi}{2(1 + \cot^2 \varphi)},$$

$$X_S(\varphi) = 1 - \frac{1}{1 + \tan \varphi},$$

$$Y_S(\varphi) = 1 - \frac{1}{1 + \cot \varphi},$$

with  $\varphi \in [0, \pi/2]$  and  $V(\varphi) = V(\varphi - \pi/2)$  for  $\varphi \in ]\pi/2, \pi]$ . The three functions for directions between 0 and  $\pi/2$  are shown in **Figure 1** (the angles are measured in degrees for the sake of lucidity). The D1-Operator damps the amplitudes by up to 11.6% (for the edge directions  $\pi/4$  and  $3\pi/4$ ). The D2-Operator amplifies the amplitudes by up to 6.1%. Finally, the S-Operator damps the amplitudes by up to 29.3%! The amplitude distortions of the D2-Operator may be tolerable in most practical applications, but the distortions caused by the operators D1 and S seem to be quite severe.

The edge direction  $\varphi$  is calculated correctly by all of the three operators. After tabulating  $V(\varphi)$  for discrete angles  $\varphi$  the amplitude-distortions can be compensated with a single division of the calculated amplitudes by  $V(\varphi)$ . This simple modification of the operators D1, D2 and S leads to the new operators MD1, MD2 and MS.

### 3: Experimental Results

In the practical part of our examinations the discrete forms of the operators were applied to synthetic, noisy step edges with distinct directions. At the top of the picture, **Figure 2** shows a cut along a line of the image. Be-

low the responses of the original and the modified operators are presented. It can be seen clearly that the theoretically predicted amplitude-distortions of the operators D1, D2 and S show up in the experiments, too. On the other hand, the new operators MD1, MD2, and MS no longer produce any systematic error in the calculated amplitudes. In case of the operators D1 and D2 the continuous distortion functions  $V_{D1}(\varphi)$  and  $V_{D2}(\varphi)$  could be used immediately for the mentioned modification of the operators. **Table 1** proves the conformity of the theoretically predicted distortions and the errors measured in our experiments. The table is based on a set of twenty noisy test images. The amplitude-distortions produced by the discrete S-Operator were found to be less severe than suspected, leading at first to an over-compensation of the errors. This discrepancy between theoretical prediction and discrete practice can be traced back to errors in the discretisation of the impulse response function of the filter: The discretisation of Shen's edge filter  $f_S(z)$  is more critical than the discretisation of Deriche's filters due to its unsteadiness in the origin. This is why  $V_S(\varphi)$  was moderately modified based on measurements in the noise-free test image (see [7]). The final form of the MS-Operator has a performance the quality of which is similar to the operators MD1 and MD2 (see **table 1**), although we observed a slightly higher sensitiveness to noise in other experiments. Moreover, the MS-Operator (and the S-Operator it is based on) tended, as we expected, to produce multiple responses to one edge and thus occasionally detected spurious edges.

Finally, the results of a comparison of the recursive operators MD1, MD2, and MS on one hand and the DG-Operator (*Derivative of Gaussian*) on the other hand are presented: The latter can be constructed by plugging in the first derivative of the Gaussian function as a one-dimensional edge filter  $f(z)$  in Deriche's scheme for edge detection. This filter has been used by Canny to approximate his optimal operator. Working with relatively large catchment areas the operators MD1, MD2, and DG perform equally well. The MS-Operator does it slightly wor-

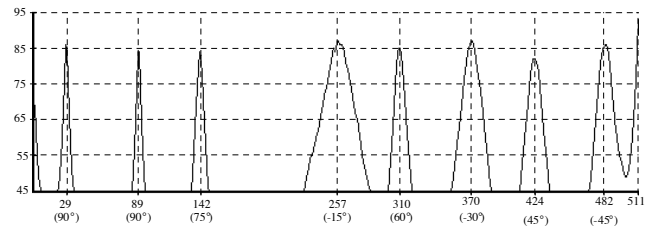
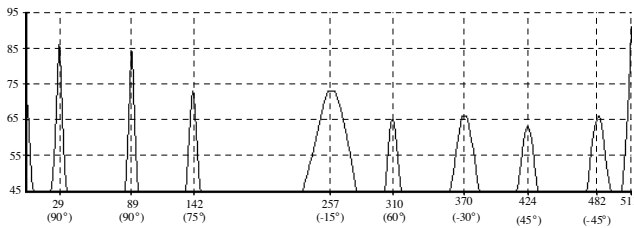
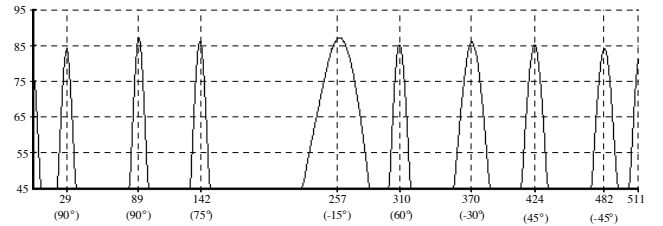
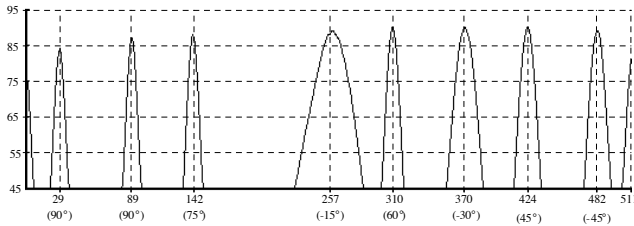
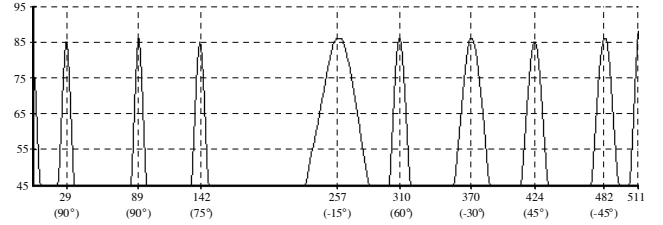
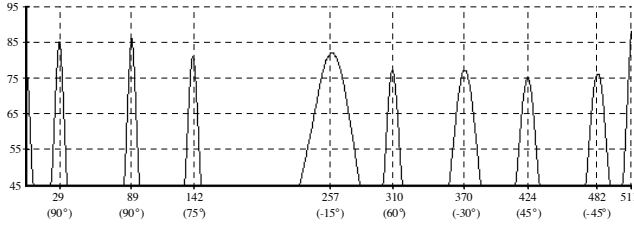
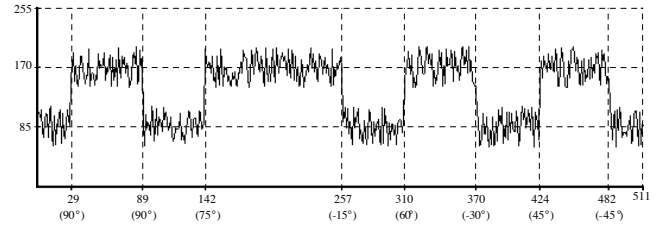
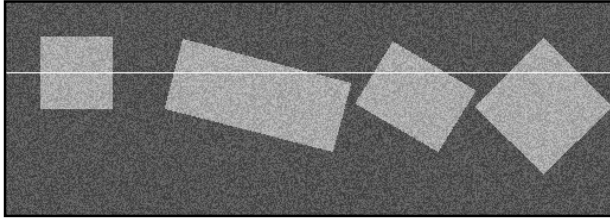


**Figure 2.** Synthetic step edges with a signal to noise ratio of 5 (upper left picture), the cut along the marked line of the test image (upper right

picture), the responses of D1 and MD1 with  $\alpha_{D1} = 0.25$  (second line), D2 und MD2 with  $\alpha_{D2} = 0.125$  (third line) and S and MS with  $\alpha_S = 0.125$  (bottom line).

$\varphi$	a)	b)	c)	d)	e)	f)	g)	h)	i)
15°	-4.5%	-4.7%	-0.1%	+2.2%	+2.1%	-0.1%	-17.2%	-14.4%	+1.2%
30°	-9.2%	-9.8%	-0.2%	+5.8%	+4.9%	-0.2%	-19.5%	-22.9%	+1.1%
45°	-11.1%	-11.6%	+0.6%	+4.8%	+6.1%	+0.6%	-23.8%	-24.4%	-0.1%
60°	-10.4%	-10.4%	+0.6%	+4.6%	+4.9%	+0.6%	-19.7%	-22.9%	-0.8%
75°	-4.8%	-4.7%	-0.4%	+3.1%	+2.1%	-0.4%	-14.6%	-14.4%	-0.8%
90°	0%	0%	0%	-0.4%	0%	-0.4%	-0.9%	0%	-0.6%

**Table 1.** The mean amplitude-distortions produced by the 2D-edge operators applied to step edges with direction  $\varphi$ .

- a) D1-Operator
- b) theoretical prediction of the error caused by D1
- c) MD1-Operator

- d) D2-Operator
- e) theoretical prediction of the error caused by D2
- f) MD2-Operator
- g) S-Operator
- h) theoretical prediction of the error caused by S
- i) MS-Operator



**Figure 3.** The MD2-Operator applied to a real world image ( $\alpha_{D2} = 0.5$ ): The original image (left), the response of the filters (middle), and the

final edge image after Non-Maximum Suppression and Hysteresis-Thresholding (right).

se. Operating with smaller catchment areas (11 x 11 pixels or less) the differences in the results of the edge detection are increasingly blurred, because the discrete impulse response functions of the filters hardly differ any more (not enough relevant sample points). Naturally, the runtime advantage of the recursively implemented operators MD1, MD2, and MS compared with the conventional DG-Operator implemented via filter masks decreases, too, if the catchment area is reduced.

In conclusion **figure 3** presents the results of an edge detection procedure using the modified operator MD2 in a real world image (512 x 512 pixels, 256 grayscales). It was gained by overlapping two interlaced video images of 256 lines each. Working with a catchment area of the used filters of about 11 x 11 pixels the resulting aliasing effects do not cause troubles (but operating with smaller catchment areas some artifacts have been observed). After recursively filtering the image a local "Non-Maximum Suppression" (i.e. a thinning operation) and a threshold operation with hysteresis (see [1]) have been performed. The overall runtime of the detection process (based on floating point arithmetic) on a Hewlett Packard 9000/700 Workstation was about 4.5 CPU seconds.

#### 4: Conclusions

Deriche's approach to edge detection is a gradient technique based on recursive filters which can be implemented very efficiently. In its original form (with Deriche's edge filter as well as Shen's edge filter embed-

ded in the scheme) it produces systematic distortions of the calculated amplitudes depending on the directions of the edges. Fortunately, these errors can be eliminated easily by the modification of the edge detection procedure presented in this paper.

#### References

- [1] J. Canny, "Finding Edges and Lines in Images"; Report, AI-TR-720, M.I.T. A.I. Lab., Cambridge, 1983.
- [2] J. Canny, "A Computational Approach to Edge Detection"; in *IEEE Transactions on Pattern Analysis and Machine Intelligence*, vol. PAMI-8, vol. 6, pp. 679-698, 1986.
- [3] S. Castan, J. Zhao und J. Shen, "Optimal Filter for Edge Detection Methods and Results"; in: Proc. of the *First European Conf. on Computer Vision, Antibes*, Lecture Notes on Comp. Science, no. 427, pp. 12-17, Springer, 1990.
- [4] R. Deriche, "Using Canny's Criteria to Derive a Recursively Implemented Optimal Edge Detector"; in: *International Journal of Comp. Vision*, vol.1, no. 2, pp. 167-187, 1987.
- [5] R. Deriche, "Optimal Edge Detection Using Recursive Filtering"; in: Proceedings of the *First International Conf. on Computer Vision, London*, pp. 501-505, 1987.
- [6] R. Deriche, "Fast Algorithms for Low-Level Vision"; in: *IEEE Transactions on Pattern Analysis and Machine Intelligence*, vol. PAMI-12, no. 1, pp. 78-87, 1990.
- [7] S. Lanser, "Detektion von Stufenkanten mittels rekursiver Filter nach Deriche"; *Diplomarbeit*, Technische Universität München, Institut für Informatik, 1991.